

Analytic continuation methods in nuclear reaction theory and indirect approaches in nuclear astrophysics

L.D. Blokhintsev

Skobeltsyn Institute of Nuclear Physics, Lomonosov
Moscow State University, Moscow, Russia

Contents

1. Nuclear vertex constants and asymptotic normalization coefficients
2. Astrophysical nuclear reaction models
3. Effects of electron screening
4. Indirect methods in nuclear astrophysics
5. Analytic continuation of effective range expansion

Asymptotic normalization coefficients (ANC) determine the asymptotics of nuclear wave functions in binary channels. ANCs are proportional to vertex constants (VC), which determine the virtual processes $A \Rightarrow B+C$.

VCS and ANCs are fundamental nuclear characteristics. They are used actively in analyses of nuclear reactions within various approaches. VCS and ANCs extracted from one process can be used for the prediction of characteristics of other processes. Comparing of empirical values of VCS and ANCs with theoretical ones enables one to evaluate the quality of a model. ANC for the channel $A \Rightarrow B+C$ determines the probability of the configuration $B+C$ in nucleus A at distances greater than the radius of nuclear interaction.


Thus **ANCs** arise naturally in cross sections of nuclear reactions between charged particles at low energies, in particular, of astrophysical nuclear reactions.

Note: Due to the Coulomb barrier cross sections at astrophysical energies are so small that their direct measurement in laboratories is very difficult, or even impossible.

Definition and Properties of ANCs and NVCs

$$I_{ABC}(LS;r) \Big|_{r \rightarrow \infty} \rightarrow C_{ABC}(LS) e^{-\kappa r} / r; \quad \kappa^2 = 2\mu\varepsilon, \quad \varepsilon = m_B + m_C - m_A. \quad (1)$$

$I_{ABC}(LS;r)$ – radial overlap integral of wave functions of A, B, C.

Coulomb interaction  $e^{-\kappa r} \rightarrow W_{-\eta, L+1/2}(2\kappa r)$

$\eta = Z_B Z_C e^2 \mu / \kappa$ - Coulomb parameter.

NVC $G_{ABC}(LS)$ is the on-shell matrix element of the virtual $A \leftrightarrow B+C$ process in the given partial-wave state LS . It is related to the amplitude of elastic BC scattering:

$$\text{res } \langle LS | M^{J_A} | LS \rangle |_{E=-\varepsilon} = (-1)^L G_{ABC}^2(LS)$$

G_{ABC} and C_{ABC} are interrelated:

$$G_{ABC}(LS) = -(\pi N_{BC})^{1/2} C_{ABC}(LS) / \mu.$$

N_{BC} arises due to the identity of nucleons.

$$1 \leq N_{BC} \leq \frac{(A_B + A_C)!}{A_B! A_C!}$$

Often N_{BC} is included into C_{ABC} .

NB! The asymptotics (1) can be rigorously proved for two-body systems only. For three- and more particle systems the asymptotics of overlap integrals may differ from (1) ('anomalous asymptotics'). (L.B. Yad. Fiz. 1981. V.34. P.944).

Considering the Fourier component $I(q)$ of the overlap integral $I(r)$ one gets

$$I(r) |_{r \rightarrow \infty} = c_0 e^{-\kappa r} / r + c_1 e^{-\kappa_1 r} / r^p, \quad p > 1, \quad (2)$$

where $i\kappa_1$ is the nearest to the origin singular point of the vertex function $G(q)$ for the $a \rightarrow b + c$ vertex. If $\kappa_1 < \kappa$, then the second term in (2) dominates at $r \rightarrow \infty$.

Consider the diagram of Fig. 1, which contributes to $G(q)$. It results from the Faddeev expansion in the simplest three-body model, in which a consists of d, f and c , b is a bound state of d and f , and e is a bound state of f and c .

For that diagram $p = 2$ and the singular point is:

$$q = i\kappa_1 = i \frac{m_b}{m_d} (\kappa_{ade} + \kappa_{bdf}), \quad \kappa_{ijk} = 2\mu_{jk} \varepsilon_{ijk}, \quad \varepsilon_{ijk} = m_j + m_k - m_i. \quad (3)$$

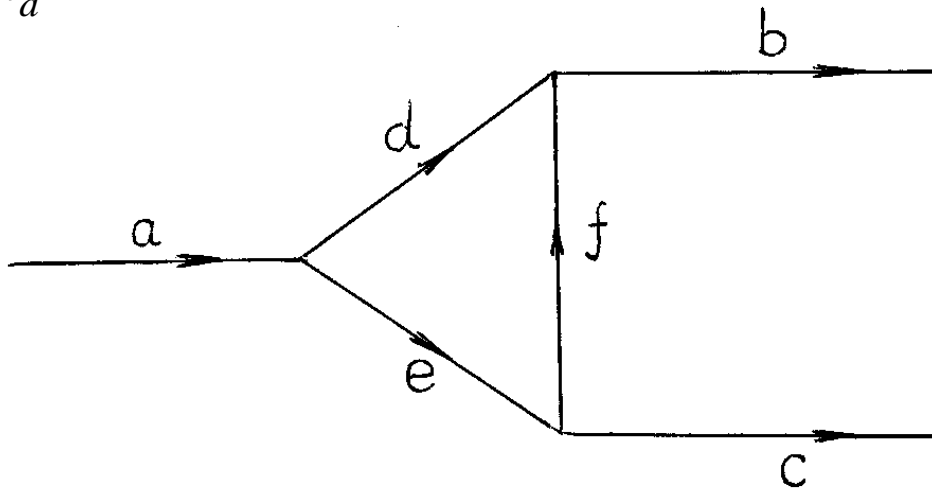


Fig. 1

At any ε_{abc} the 'anomalous' condition $\kappa_1 < \kappa$ could be satisfied if ε_{ade} and ε_{bdf} are sufficiently small.

Configuration representation

Consider the same system c, d, f with bound states $a = \{cdf\}$, $b = \{df\}$, and $e = \{fc\}$.

Let $\psi_a(\mathbf{r}, \boldsymbol{\rho})$, $\varphi_b(\boldsymbol{\rho})$, $\varphi_e(\mathbf{r}_{fc})$ be the inner wave functions of a, b , and e ($\mathbf{r} = \mathbf{r}_{bc}$, $\boldsymbol{\rho} = \mathbf{r}_{df}$).

The overlap integral for $a \rightarrow b + c$ is

$$I(\mathbf{r}) = \int \psi_a(\mathbf{r}, \boldsymbol{\rho}) \varphi_b^*(\boldsymbol{\rho}) d\boldsymbol{\rho}. \quad (4)$$

According to S.P.Merkuriev. Yad.Fiz. 1974. V. 19. P. 447 at $r \rightarrow \infty$ and finite values of ρ $\psi_a(\mathbf{r}, \boldsymbol{\rho})$ possesses the following asymptotics (for the short-range interaction)

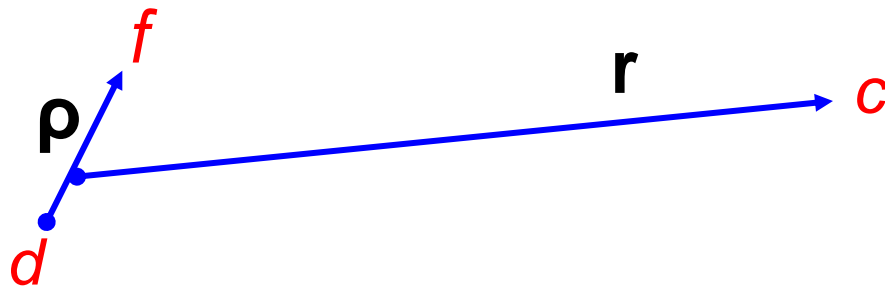
$$\psi_a(\mathbf{r}, \boldsymbol{\rho}) \rightarrow \varphi_b(\boldsymbol{\rho}) \frac{e^{-\kappa r}}{r} u_{bc}(\mathbf{n}_{bc}), \quad (5)$$

where $u_{bc}(\mathbf{n}_{bc})$ is the certain function of angular variables.

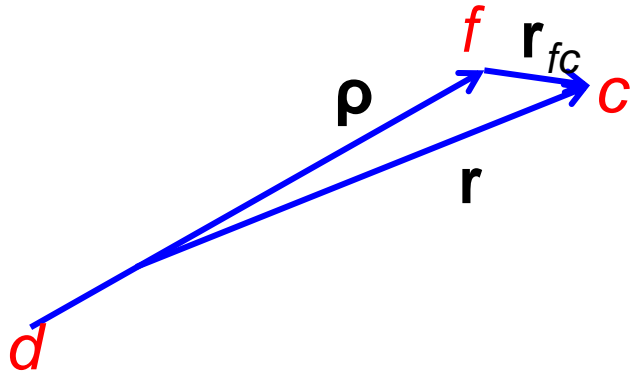
At finite $\boldsymbol{\rho}$ $\varphi_b(\boldsymbol{\rho})$ is generally finite. Hence, inserting (5) into (4), one sees that the contribution $I_1(\mathbf{r})$ to the overlap integral $I(\mathbf{r})$ from the domain Ω_1 of finite $\boldsymbol{\rho}$ possesses the normal asymptotics

$$I_1(\mathbf{r}) \rightarrow \text{const} \cdot \frac{e^{-\kappa r}}{r} u_{bc}(\mathbf{n}_{bc}), \quad r \rightarrow \infty. \quad (6)$$

Ω_1 domain corresponds to the configuration:



Consider now the domain Ω_2 of $\boldsymbol{\rho}$, in which r_{fc} is finite.



$$\mathbf{r}_{fc} = \mathbf{r} - \frac{m_d}{m_b} \boldsymbol{\rho}, \quad \mathbf{r}_{de} = \frac{m_c}{m_e} \mathbf{r} + \frac{m_f m_a}{m_3 m_b} \boldsymbol{\rho},$$

Hence at $r \rightarrow \infty$ for all $\boldsymbol{\rho} \in \Omega_2$ $\rho \rightarrow \infty$ and

$$\boldsymbol{\rho} \approx \frac{m_b}{m_d} \mathbf{r}, \quad \mathbf{r}_{de} \approx \boldsymbol{\rho} \approx \frac{m_b}{m_d} \mathbf{r}, \quad r \rightarrow \infty. \quad (7)$$

Analogously to (5) at $r \rightarrow \infty$ and finite values of r_{fc} one obtains

$$\psi_a(\mathbf{r}, \rho) \rightarrow \varphi_e(\mathbf{r}_{fc}) \frac{e^{-\kappa_{ade} r_{de}}}{r_{de}} u_{de}(\mathbf{n}_{de}), \quad (8)$$

Besides, at $\rho \rightarrow \infty$

$$\varphi_b(\rho) \rightarrow (e^{-\kappa_{bdf} r_{df}} / r_{df}) u_{df}(\mathbf{n}_{df}). \quad (9)$$

It follows from (8), (9), and (7) that at $\rho \rightarrow \infty$ the contribution of Ω_2 to $I(\mathbf{r})$ (4) is

$$I_2(\mathbf{r}) \rightarrow \{ \exp[-(m_b / m_d)(\kappa_{bdf} + \kappa_{ade})r] / r^2 \} \chi(\mathbf{n}) = (e^{-\kappa_1 r} / r^2) \chi(\mathbf{n}), \quad (10)$$

$\chi(\mathbf{n})$ depends on angles only.

Thus the asymptotics of $I_2(\mathbf{r})$ coincides exactly with the anomalous asymptotics due to diagram 1. At $\kappa > \kappa_1$ the asymptotics of the full overlap integral $I(\mathbf{r})$ coincides with the asymptotics (10). This result is generalized easily to the presence of the Coulomb interaction.

Methods of determination of ANCs and VCs

1. Microscopic calculations \Rightarrow very difficult

1a. Coordinate representation \Rightarrow asymptotical region \Rightarrow
small values of wave functions \Rightarrow low accuracy

1b. Momentum representation \Rightarrow continuation to imaginary
values of momenta

The only reliable calculation of ANCs for an α particle \Rightarrow

M.Viviani, A.Kievsky, M.Rosati (PRC 71, 024006 (2005)).

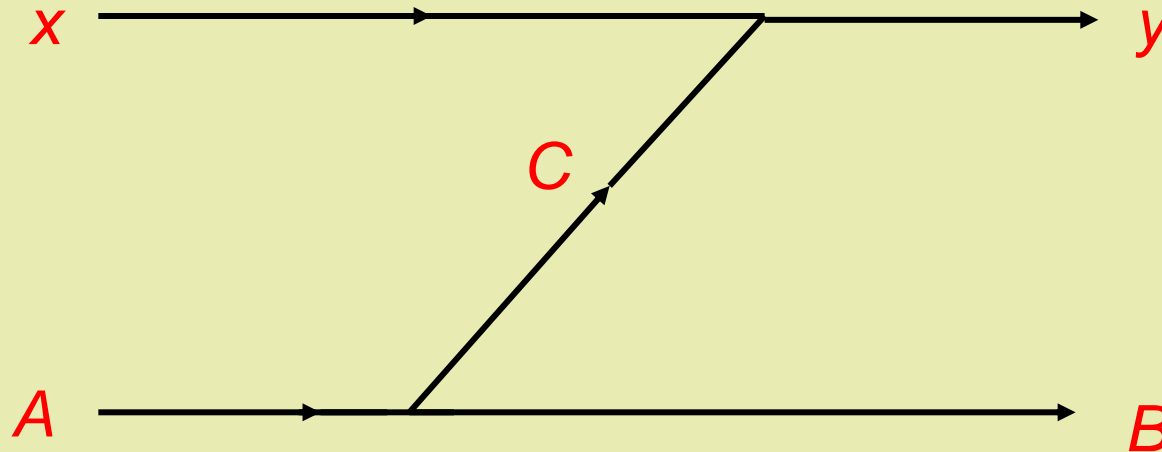
2. Analysis of experimental data

2a. Data on bound nuclear states cannot be used since VCs and ANCs are independent nuclear characteristics.

Alternative way \Rightarrow analysis of scattering and reactions

2b. Analysis of data on transfer reactions proceeding through the pole mechanism

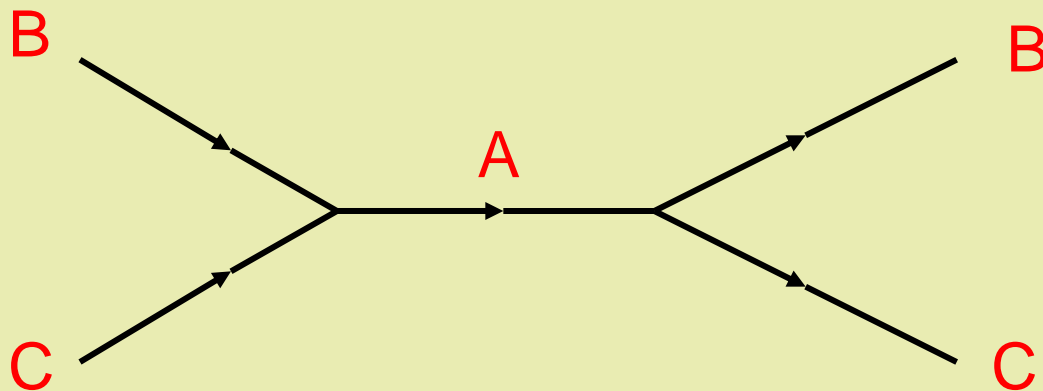
$A(x,y)B$



The cross section of this reaction possesses the 2nd order pole at $z = z_0$ ($z = \cos \theta$, $|z_0| > 1$). If one extrapolates the experimental values of $(z - z_0)^2 \sigma(z)$ to the pole position ($\sigma(z)$ is the differential cross section), one immediately obtains the value of $|G_{ABC} G_{yxC}|^2$.

Note. Account of the Coulomb interaction in the vertices of the diagram turns a pole to a branch point.

2c. Extrapolation in energy E of the partial-wave amplitude of elastic BC scattering (obtained by the phase-shift analysis) to the pole corresponding to the bound state A .



2d. For peripheral nuclear reactions VC could be obtained from the DWBA analysis of differential cross sections .

The problem of using continuum-state data to obtain information on bound-state characteristics is not trivial !!!

“Bound-state properties cannot be extracted from the phase shifts of a single partial wave, as a matter of principle”.

J-M. Sparenberg (Phys. Rev. C, **69**, 034601 (2004))

This assertion is based on the existence of phase-equivalent potentials (PEP). Different PEPs lead to coinciding phase shifts $\delta_L(E)$ but properties of the bound states for a given L are different.

Inverse scattering problem: to restore a local potential one needs:

- i) $\delta_L(E)$, $0 \leq E < \infty$.
- ii) $2N_L$ parameters (N_L – number of bound states for a given L).
 $2N_L \rightarrow N_L$ binding energies and N_L ANCs.

Methods of constructing PEP's

- 1) Bargmann potentials (R.Newton, Scattering Theory).
- 2) Supersymmetric transformation (E.Witten (1981)).

Supersymmetric transformation can be used to construct PEP, which differs from the initial potential by any modification of the bound spectrum. A bound state can be added or suppressed; its binding energy and/or ANC can be modified.

Inference: Within the formal potential approach with arbitrary potentials and without any additional conditions, it is impossible to determine unambiguously characteristics of bound states knowing only $\delta_L(E)$.

The way to resolve the ambiguity problem:

The natural requirement that amplitudes of processes are **analytic functions** of their kinematic variables.

Microcausality principle \implies Analyticity

Using analyticity and knowing the partial-wave **BC** scattering amplitude $f_L(E)$ on some segment of the real positive semiaxis, one can continue analytically $f_L(E)$ to the unphysical region $E < 0$ and obtain both the position of the pole $E = -\varepsilon < 0$ and the residue of $f_L(E)$ at that pole, that is, **VC** and **ANC**.

Note. We discuss the principal side of the problem and not the practical ways of analytic continuation.

Two-body potential scattering

Knowing ε , ANC C_{ABC} , and $f_L(E)$ at $0 \leq E < \infty$, one can construct unambiguously a local potential $V(r)$ using methods of the inverse scattering problem. As a result, the unique “analytic” potential would be selected out of set of PEPs, which leads to the needed analytic properties of the scattering amplitude. That potential describes all bound and continuum states of a given system.

Characteristics of a bound state obtained by the direct analytic continuation of $f_L(E)$ from $E \geq 0$ to $E < 0$ may differ from the characteristics found by solving the bound state problem with the potential which describes correctly $f_L(E)$ at $E \geq 0$. Why?

In potential scattering theory

$$f_L(k) = -\frac{\mu}{2\pi} \int_0^{\infty} dr \varphi_L(kr) V(r) \psi_L(kr)$$

If k is continued to the complex plane, the terms $e^{2|\text{Im}k|r} V(r)$ arise in the integrand, which lead to the divergence of the integral if $V(r)$ does not decrease rapidly enough at $r \rightarrow \infty$.

$f_L(k)$ in the above form can be analytically continued to $k = ik$ ($E = -\varepsilon$) if (R.Newton, Scattering Theory):

$$\int_0^{\infty} dr r |V(r)| e^{2kr} < \infty \quad (L = 0).$$

Other possibilities of analytic continuation of amplitudes

- the explicit form of $f_L(E)$ at $E \geq 0$ is known
- one succeeds in approximating $f_L(E)$ at $E \geq 0$ by a certain analytic expression accurately enough

Consider a trivial example:
$$\varphi(z) = \int_0^{\infty} e^{(a-z)t} dt$$

$\varphi(z)$ initially is defined only at $\text{Re } z > \text{Re } a$ since if this inequality is violated, the integral diverges.

On the other hand, the integration can be performed explicitly:

$$\varphi(z) = \frac{1}{z - a}$$

. This expression defines the function, which is analytic in the whole complex z plane with a pole at $z = a$.

Instructive example of a Bargmann-type potential

(R.Newton, Scattering theory)

$$V_d(r) = -\frac{\kappa}{\mu} \frac{d}{dr} \left[\operatorname{sh}(br) \frac{g_d(\kappa, r)}{g_d(\kappa + b, r) - g_d(\kappa - b, r)} \right], \quad b > \kappa.$$

$$g_d(x, r) = x^{-1} [e^{-\kappa r} + d \operatorname{sh}(xr)].$$

Normalized bound-state wave function ($\varepsilon = \kappa^2/2\mu$):

$$\varphi_d(r) = 2 \sqrt{\frac{\kappa d}{b^2 - \kappa^2}} \frac{\operatorname{sh}(br)}{g_d(\kappa + b, r) - g_d(\kappa - b, r)}$$

S wave scattering amplitude does not depend on **d**:

$$f(k) = \frac{e^{2i\delta} - 1}{2ik} = \frac{1}{k \operatorname{ctg} \delta - ik} = \frac{b + \kappa}{-b\kappa + k^2 - i(b + \kappa)k}$$

$f(k)$ can be analytically continued to the pole $k = i\kappa$ and ANC is expressed through the residue at that pole:

$$C = \left[\frac{2\kappa(b + \kappa)}{b - \kappa} \right]^{1/2}$$

On the other hand, the expression for ANC depending on the parameter d can be obtained from the explicit form of φ_d :

$$C_d = \left[\frac{4\kappa(b + \kappa)}{d(b - \kappa)} \right]^{1/2}$$

$C_d = C$ at $d = 2$ only.

Why $d = 2$ is special? Because the asymptotics of $V_d(r)$ at $d = 2$ is special:

$$V_d(r)_{r \rightarrow \infty} \rightarrow \begin{cases} -V_1 \cdot e^{-2\kappa r}, & d \neq 2, \\ -V_2 \cdot e^{-2br}, & d = 2. \end{cases}$$

Since $b > \kappa$, the necessary “analyticity” condition:

$$\lim_{r \rightarrow \infty} V_d(r) e^{2\kappa r} = 0$$

is satisfied at $d = 2$ only.

Thus the analytic continuation of the amplitude $f(k)$ to the region of imaginary k allows one to select from the set of PEP $V_d(r)$ the only “analytic” potential corresponding to $d = 2$ and find the correct value of the ANC C .

PEPs obtained by the supersymmetric transformation acquire the singularity of the type $1/r^2$ at the origin and, as well as $V_d(r)$ at $d \neq 2$, do not satisfy the integral analyticity condition.

$$\int_0^{\infty} dr r |V(r)| e^{2\kappa r} < \infty.$$

Reactions with composite systems (nuclei)

Description of elastic nucleon-nucleus or nucleus-nucleus scattering in the two-body potential approach \implies corresponding potential is complex, nonlocal and energy- and angular momentum dependent.

Nevertheless, one can still use analytic continuation of $f_L(E)$ to $E < 0$ to find the binding energy and the VC and ANC. Analytic continuation can be performed in different ways.

In the work (L.B., V.I.Kukulin *et al.*, PRC 48, 2390 (1993))
VC $G_{6\text{Li}\alpha d}$ and ANC $C_{6\text{Li}\alpha d}$ for the **S** state of ${}^6\text{Li}$ were found in
two ways.

1. Analytic approximation of experimental values of $k \cot \delta$
using Pade approximants and subsequent continuation to $E < 0$.
2. Constructing the effective two-body $d\alpha$ potential $V_{d\alpha}(r)$
describing experimental δ and finding the two-body bound-
state wave function for this potential. $V_{d\alpha}(r)$ was written as a
sum of oscillatory functions and satisfied the necessary
analyticity conditions.

The results of two different methods are in close agreement.

Important comment

In the general case, when B and/or C are composite systems, ANC C_{ABC} corresponds to the overlap integral $I_{ABC}(r)$, which is normalized not to 1 but to the spectroscopic factor S_{ABC} .

However, if ANC is found in the two-body model, the corresponding two-body bound-state wave function should be normalized to 1. Normalizing this function to the independently determined spectroscopic factor is incorrect.

Inference

1. Using the fundamental analyticity property of scattering amplitudes and analytic continuation methods allows one to obtain information on characteristics of nuclear bound states (including ANCs) from the phase shift data. Thus the ambiguity related to the existence of phase-equivalent potentials is removed.

2. The most effective method of analytic continuation \Rightarrow analytic approximation of the experimental values of $k \cot \delta$.

3. If the continuation is performed by fitting a two-body potential, one should use the potential which decreases rapidly enough at $r \rightarrow \infty$. One should put the spectroscopic factor equal to 1.

Selected problems of nuclear astrophysics

Introduction

Nuclear reactions in stars and stellar explosions are responsible for the ongoing synthesis of chemical elements. Nuclear physics plays an important role as it determines the signatures of isotopic and elemental abundances found in the spectra of stars, novae, supernovae, and X-ray bursts.

The rapid neutron capture process (r process) is responsible for the existence of about half of the stable nuclei heavier than iron. Capture cross sections for most of the nuclei involved are hard if not impossible to measure in the laboratory and indirect experimental approaches have to be employed to gather the relevant nuclear structure information. The same concerns (p,γ) and (p,α) reactions.

The quantities used in nucleosynthesis calculations are reaction rates. A thermonuclear reaction rate is a function of the density of the interacting nuclei, their relative velocity and the reaction cross section. Extrapolation procedures are often needed to derive cross sections in the energy or temperature region of astrophysical relevance. While non-resonant cross sections can be extrapolated rather well to the low-energy region, the presence of continuum, or sub-threshold resonances, can complicate these extrapolations.

As an example of an important astrophysical reaction one may mention ${}^7\text{Be}(p, \gamma){}^8\text{B}$, which plays a major role for the production of high energy neutrinos from the β -decay of ${}^8\text{B}$. These neutrinos come directly from the center of the Sun and are ideal probes of the Sun's structure. The reaction ${}^{12}\text{C}(\alpha, \gamma){}^{16}\text{O}$ is extremely relevant for the fate of massive stars. It determines if the remnant of a supernova explosion becomes a black hole or a neutron star. These two reactions are only two examples of a large number of reactions, which are not yet known with the accuracy needed in astrophysics.

Thermonuclear cross-sections and reaction rates

The number of reactions between a target j and a projectile k per unit volume and time can be expressed as $r = \sigma v n_j n_k$,

or, more generally, by

$$r_{jk} = \int \sigma v d^3 n_j d^3 n_k. \quad (1)$$

Here σ – cross section, v – relative velocity, n_j and n_k – number densities. For nuclei j and k in an astrophysical plasma, obeying a Maxwell-Boltzmann distribution,

$$d^3 n_j = n_j \left(\frac{m_j}{2\pi kT} \right)^{3/2} \exp\left(-\frac{m_j v_j^2}{2kT} \right) d^3 v_j. \quad (2)$$

□

Using (2), one can rewrite (1) as:

$$r_{jk} = \langle \sigma v \rangle_{jk} n_j n_k, \quad \langle \sigma v \rangle_{jk} = \left(\frac{8}{\pi \mu_{jk}} \right)^{1/2} (kT)^{-3/2} \int_0^\infty E \sigma(E) \exp\left(-\frac{E}{kT} \right) dE, \quad (3)$$

where $\langle \sigma v \rangle_{jk}$ is the average over the temperature distribution, μ_{jk} is the reduced mass.

Charged particles

Experimentally, it is more convenient to work with the astrophysical **S** factor

$$S(E) = E\sigma(E)\exp(2\pi\eta), \quad \eta = Z_j Z_k e^2 / v. \quad (4)$$

(3) can be written as

$$\langle \sigma v \rangle_{jk} = \left(\frac{8}{\pi\mu_{jk}} \right)^{1/2} (kT)^{-3/2} \int_0^\infty S(E) \exp\left(-\frac{E}{kT} - \frac{b}{E^{1/2}} \right) dE, \quad b = 2\pi\eta E^{1/2}. \quad (5)$$

If one assumes that **S(E)** is a constant, then the integrand in (5) is maximal at the Gamow energy

$$E_0 = (bkT/2)^{2/3}. \quad (6)$$

Measurements of cross sections at low energies are difficult and the extrapolation from higher energies can be complicated by the presence of unknown resonances.

Nuclear reactions at the Sun

The Sun belongs to the main-sequence stars, the energy of which is due to the *pp*- и *CNO*- cycles

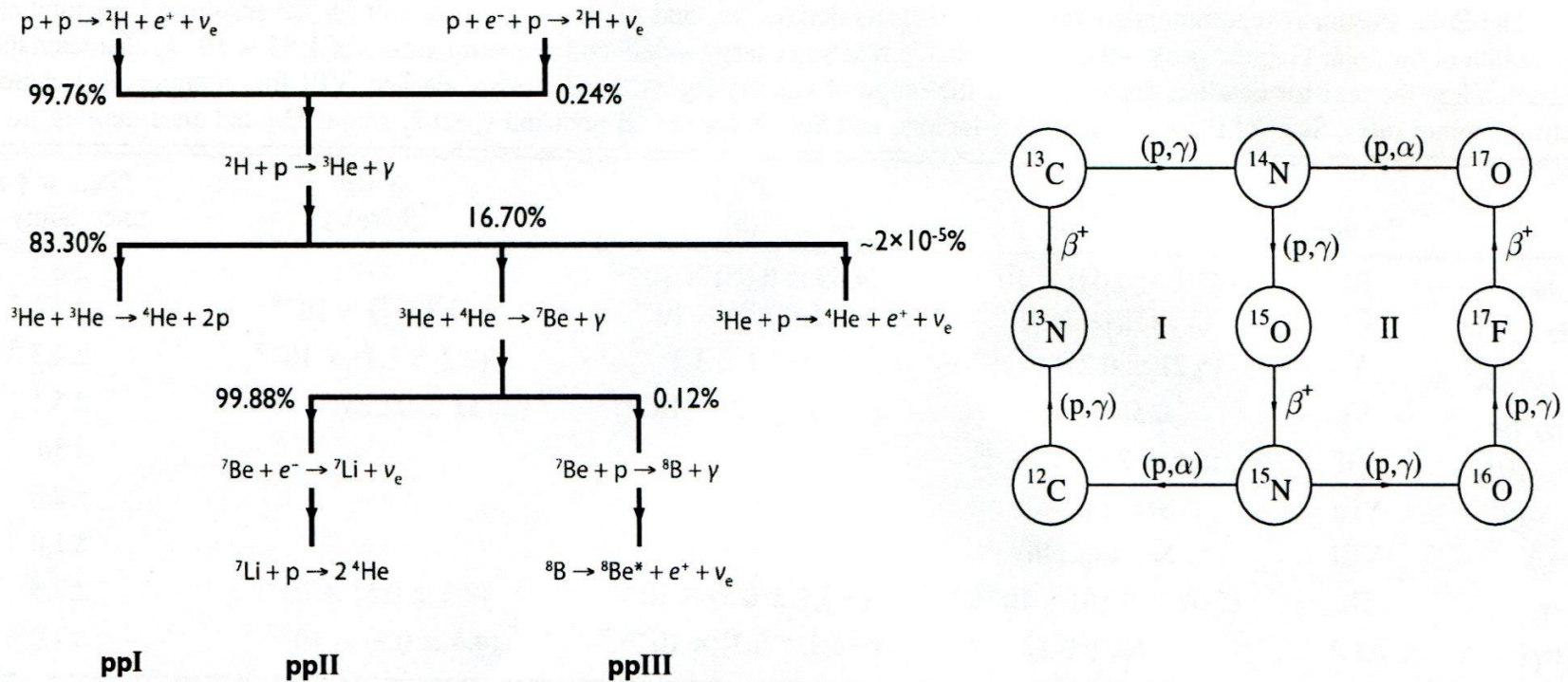


Fig.1

According to the Standard Sun model **~99%** of the Sun energy is generated by the ***pp***-cycle, the ultimate result of which is the transmutation of 4 protons into helium

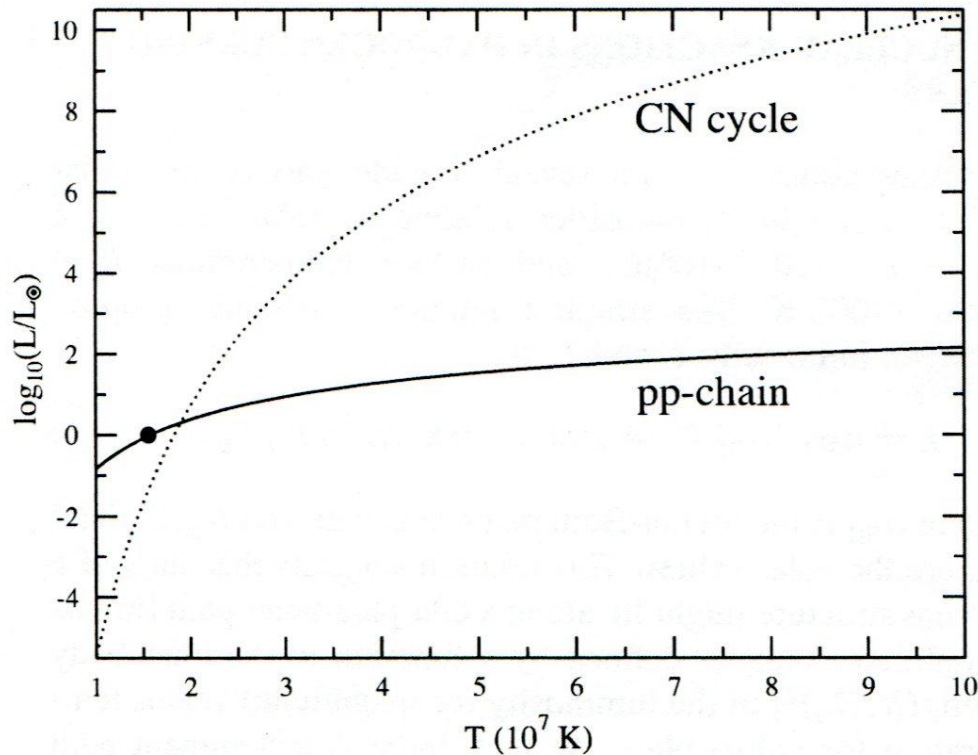


Fig. 2

Explosive nuclear burning in astrophysical environments produces short-lived, exotic nuclei, which again can be targets for subsequent reactions. In addition, it involves a very large number of stable nuclei, which are still not fully explored by experiments. Thus, it is necessary to be able to predict reaction cross-sections and thermonuclear rates with the aid of theoretical models, moreover that a direct cross-section measurement is often not possible with existing experimental techniques. For the reliable extrapolation down to the stellar energies of the cross sections measured at the lowest possible energies in the laboratory such extrapolations should have as strong a theoretical foundation as possible. Theory is even more mandatory when excited or unstable nuclei are involved in the entrance channel.

Nuclear reaction models

1. Potential models assume that the physically important degrees of freedom are the relative motion between structureless nuclei in the entrance and exit channels. Interaction between them is described by the optical potential (usually in the Woods-Saxon form). DWBA is used practically for all astrophysical nuclear reactions. The only microscopic information is introduced in terms of spectroscopic factors and parameters of the optical potential. Deficiency – the optical parameters cannot be determined unambiguously.

2. In microscopic models, nucleons are grouped into clusters and the completely antisymmetrized relative wave functions between the various clusters are determined by solving the Schrödinger equation for a many-body Hamiltonian with an effective nucleon-nucleon interaction. Typical cluster models are based on the Resonating Group Method (RGM) or the Generator Coordinate Method (GCM). They result in a complicated set of coupled integro-differential equations.

Modern nuclear shell-model calculations, such as the Monte-Carlo shell model, or the no-core shell model, are able to provide the wave functions for light nuclei. But so far they cannot describe scattering wave functions with a sufficient accuracy.

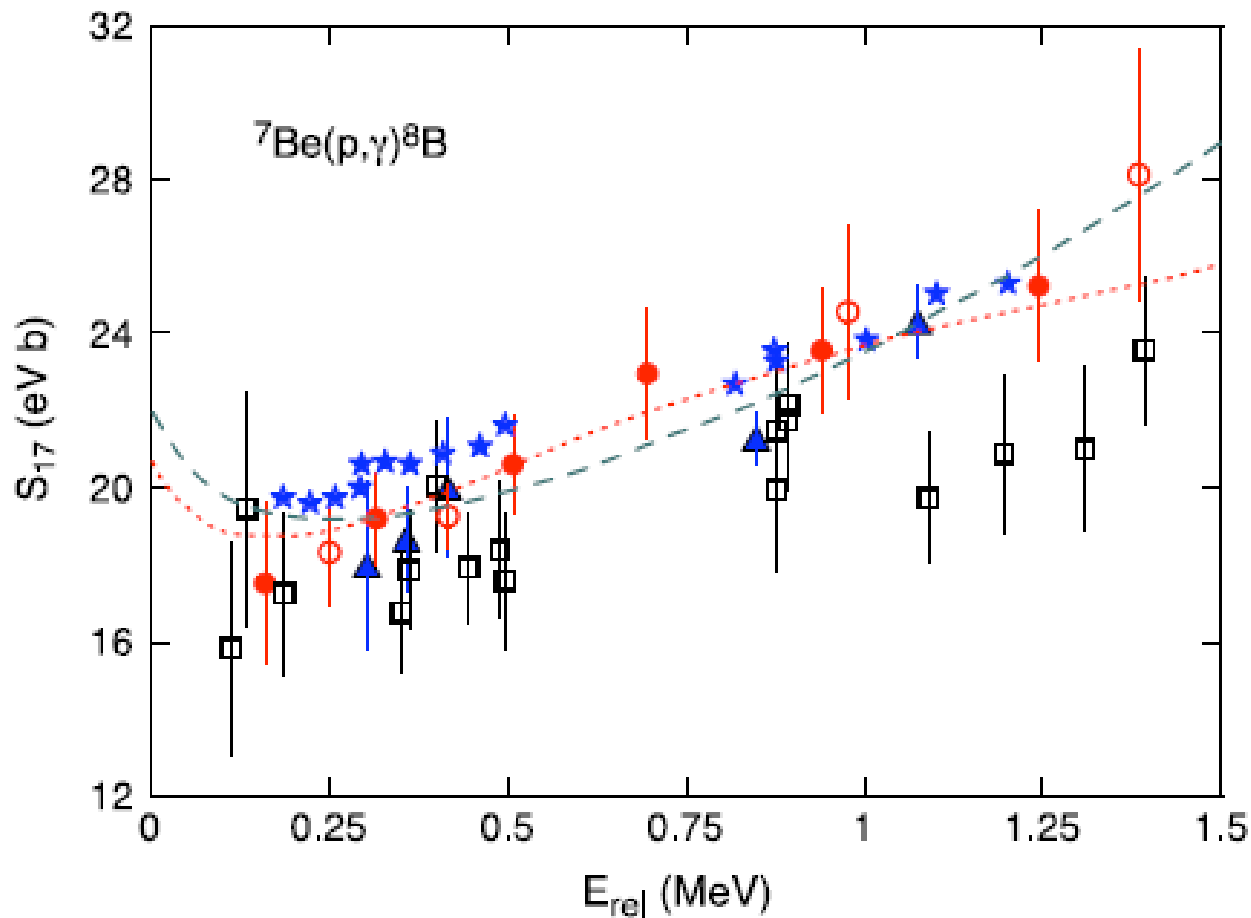


Fig. 3

Green dashed line - no-core shell model, red dotted line – RGM. Expt. Data – from 8 different works. It is evident that both theory and experiment need improvement for this important reaction.

Field theories adopt a completely independent approach for nuclear physics calculations in which the concept of nuclear potentials is not used. The basic method of field theories is to start with a Lagrangian for the fields, from which one constructs the Feynman diagrams and make practical calculations.

Effective field theory (EFT) by-passes complications of quantum chromodynamics (QCD) using the expansion over the small parameter, which is determined by the ratio of short-range and long-range (or “light” and “heavy”) scales. Practically for the NN interaction that parameter is

$$p = \frac{(1/a, B, k)}{\Lambda}, \quad (8)$$

where a – NN scattering length, B and k – typical binding energy and nucleon momentum. «Heavy» scale is determined by the pion mass: $\Lambda \sim m_\pi \sim 140$ MeV.

Reaction rates dominated by the contributions from a few resonant or bound states are often extrapolated to energies of astrophysical interest in terms of R -matrix fits. The appeal of these methods rests on the fact that analytical expressions can be derived from underlying formal reaction theories that allow for a rather simple parameterization of the data. However, the relation between the parameters of the R -matrix model and the experimental data is only quite indirect.

A large fraction of the reactions of interest proceed through compound systems that exhibit high enough level densities for statistical methods to provide a reliable description of the reaction mechanism. The theoretical treatment of nuclear reactions leading to formation and decay of compound nuclei was developed by Ewing and Weisskopf based on two ideas: (a) the compound nucleus formation independence hypothesis as proposed by Niels Bohr, and (b) the reciprocity theorem, or time-reversal properties of the underlying Hamiltonian. This allows one to relate capture and decay cross sections.

Effects of electron screening

The form of the astrophysical S factor given in Eq. (4) assumes that the electric charges of nuclei are “bare” charges.

However, neither at very low laboratory energies, nor in stellar environments is this the case. In stars, the bare Coulomb

interaction between the nuclei is screened by the electrons in the plasma surrounding them. If one measures reaction rates in the laboratory, using atomic targets (always), then atomic electrons screen as well.

1. Stellar electron screening

Coulomb interaction between two charges in a neutral plasma can be written as

$$V(r) = \frac{Z_1 Z_2 e^2}{r} \exp\left(-\frac{r}{R_D}\right), \quad (9)$$

where R_D is the Debye radius, that is the distance over which the electric field of a separated charge acts in the neutral medium consisting of positive and negative charged particles. In the weak screening approximation

$$V(r) \approx \frac{Z_1 Z_2 e^2}{r} \left(1 - \frac{r}{R_D}\right) = V_b(r) + U_0, \quad U_0 = -\frac{Z_1 Z_2 e^2}{R_D}. \quad (10)$$

As a result the velocity of a reaction increases

$$\langle \sigma v \rangle_{\text{screened}} = f \langle \sigma v \rangle_{\text{bare}}, \quad f = \exp(|U_0| / kT). \quad (11)$$

2. Atomic electron screening

The laboratory screening can be evaluated in the adiabatic approximation, in which one assumes that the velocities of the electrons in the target are much larger than the relative motion between the projectile and the target nucleus. In this case, the electronic cloud adjusts to the ground-state of a temporary “molecule” consisting of two nuclei separated by a time-dependent distance $R(t)$, at each time instant t . Since the closest approach distance between the nuclei is much smaller than typical atomic cloud sizes, the binding energy of the electrons will be given by the ground-state energy of the $Z_P + Z_T$ atom. Energy conservation implies that the relative energy between the nuclei increases by

$$U_e = B(Z_p + Z_t) - B(Z_t). \quad (12)$$

U_e is the screening potential.

This energy increment enhances the fusion (tunneling) probability. Supposing that U_e/E is small and using (4) one gets

$$\sigma(E + U_e) = \exp\left[\pi\eta(E)\frac{U_e}{E}\right]\sigma(E). \quad (13)$$

The values of U_e needed to reproduce the experimental data are systematically **larger** than the theoretical ones by a factor of 2.

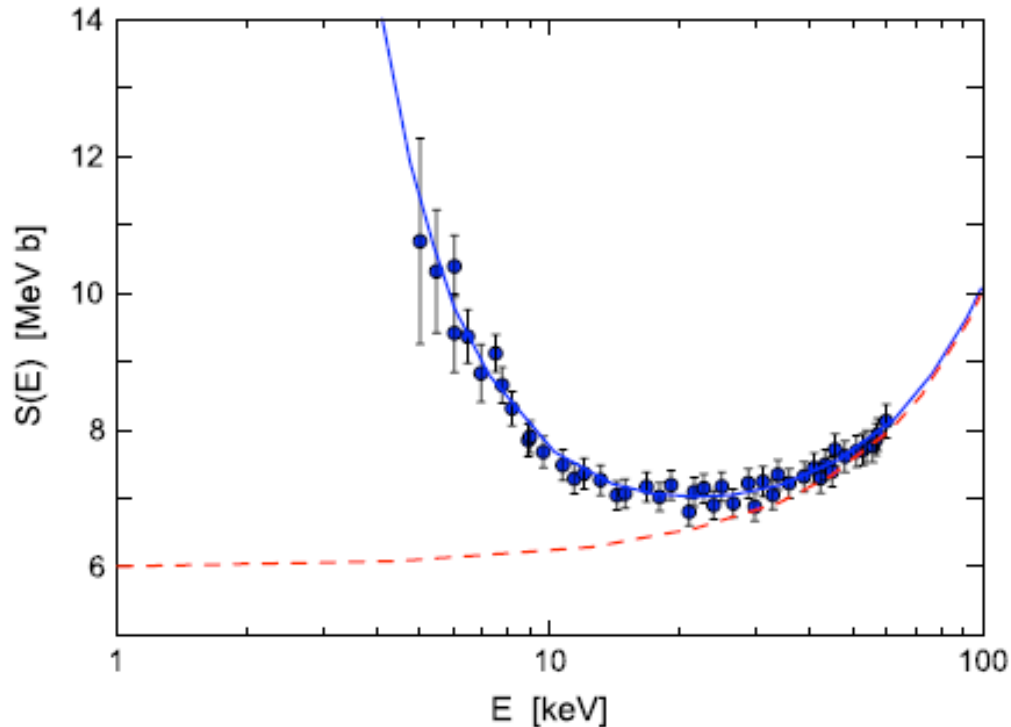


Fig. 4. Reaction ${}^3\text{He}(d,p){}^4\text{He}$. Dashed curve – bare nuclei, solid curve – screened nuclei with $U_e = 219$ eV (theory gives $U_e = 119$ eV).

Indirect methods of obtaining information on astrophysical nuclear reactions

1. Trojan horse method

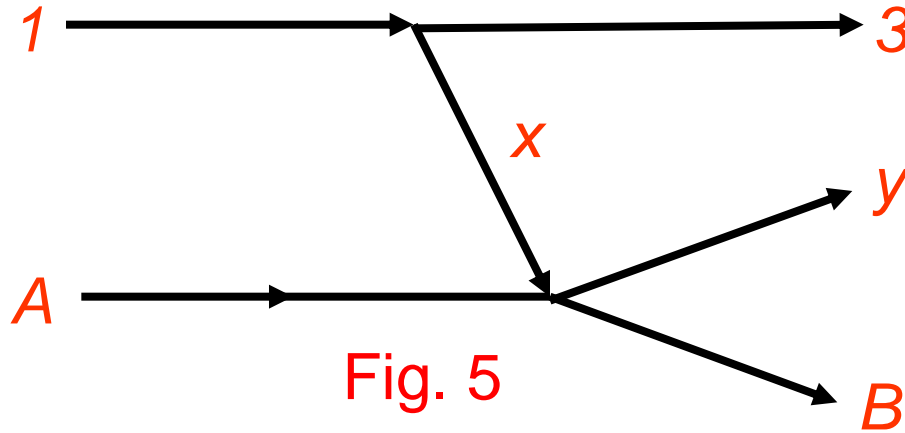
The Trojan horse (TH) method (*G.Baur, Phys. Lett. B 178 (1986)*) is an effective indirect method of determining cross sections of astrophysical binary reactions by measuring cross sections of reactions with three particles in the final state.

Let we are interested in the $A + x \rightarrow B + y$ reaction at low (astrophysical) energies, and direct measurements are not possible due to the Coulomb barrier. Consider the reaction

$1 + A \rightarrow 3 + B + y$ where $1 = 3 + x$.

Particle 1 is the Trojan horse with particle x inside it.

Consider the quasifree mechanism



At low momentum transferred from 1 to 3 , that mechanism could give the dominant contribution (or at least determine angular and energetic dependencies). The corresponding differential cross section is of the form

$$\sigma_{3diff}(A+1 \rightarrow B+y+3) = KF \cdot \psi^2(1 \rightarrow 3+x) \cdot \tilde{\sigma}_{2diff}(A+x \rightarrow B+y) \quad (14)$$

If KF and ψ^2 are known, $\tilde{\sigma}_{2diff}$ could be extracted from σ_{3diff} .

Often $1 = d$, $x = p$, $3 = n$.

$\tilde{\sigma}_2$ differs from the free cross section σ_2 by particle x being virtual (off-shell), that is $\tilde{\sigma}_2$ describes the $A + x \rightarrow B + y$ process half-off-shell.

Using the energy and momentum conservation laws at the vertices of the diagram of Fig.5, one can show that the relative momentum k of particles A and x in the initial state of the reaction $A + x \rightarrow B + y$ remains non-zero at $E_{Ax} \rightarrow 0$. Hence the Coulomb barrier factor $e^{-2\pi\eta_i}$ does not appear in the expression for $\tilde{\sigma}_2$, and it remains finite at $E_{Ax} \rightarrow 0$.

Qualitative explanation: Particle x has already overcome the Coulomb barrier in the initial state as a part of particle 1.

Note. Initial energy E_{A1} can be chosen large enough so that the reaction can be measured.

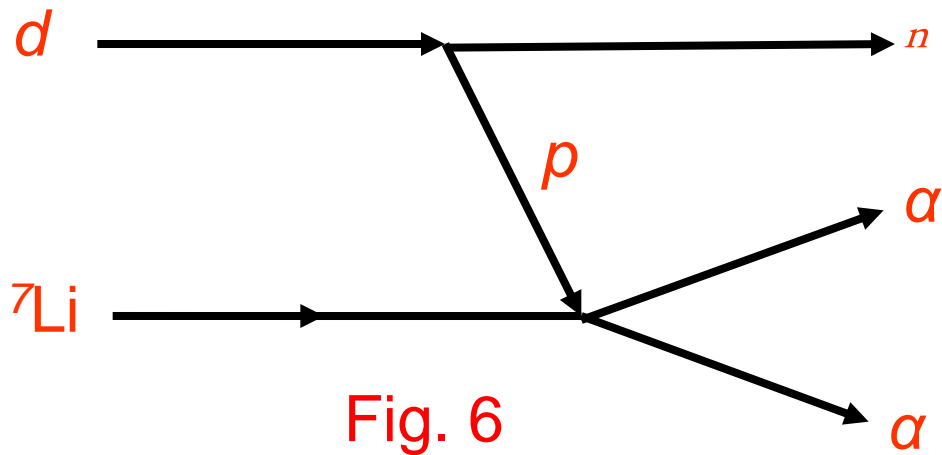


Fig. 6

1. Initial energy E_{dLi} large ($E_{Li} \sim 20$ MeV).
2. Choice of $E_{\alpha\alpha} \Rightarrow$ determining $\tilde{\sigma}_2$ at $E_{pLi} \sim 0$. ($E_{pLi} = E_{\alpha\alpha} - Q$).
3. Multiplication by the Coulomb penetration factor \Rightarrow
 $\sigma_2(E_{pLi})$ and $S(E_{pLi})$ at $E_{pLi} \sim 0$.

$$S(E) = \sigma(E) \cdot E \cdot e^{2\pi\eta}, \quad \eta = Z_1 Z_2 e^2 / \hbar v.$$

(15)

Practically the absolute value of $S(E)$ is found by the normalization to direct measurements at higher energies when the penetration factor $e^{-2\pi\eta} \approx 1$.

By comparing the cross section thus obtained with the laboratory one at lower energies one can obtain the information on electron screening effects. These effects, which are essential at very low energies, are described by multiplication of the reaction cross section on the "bare" nucleus by $e^{\pi\eta U_e/E}$, what results in increasing of the cross section (U_e is the screening potential). The Trojan horse cross section σ_b is free from screening effects, and its comparison with directly measured allows one to obtain the information on U_e .

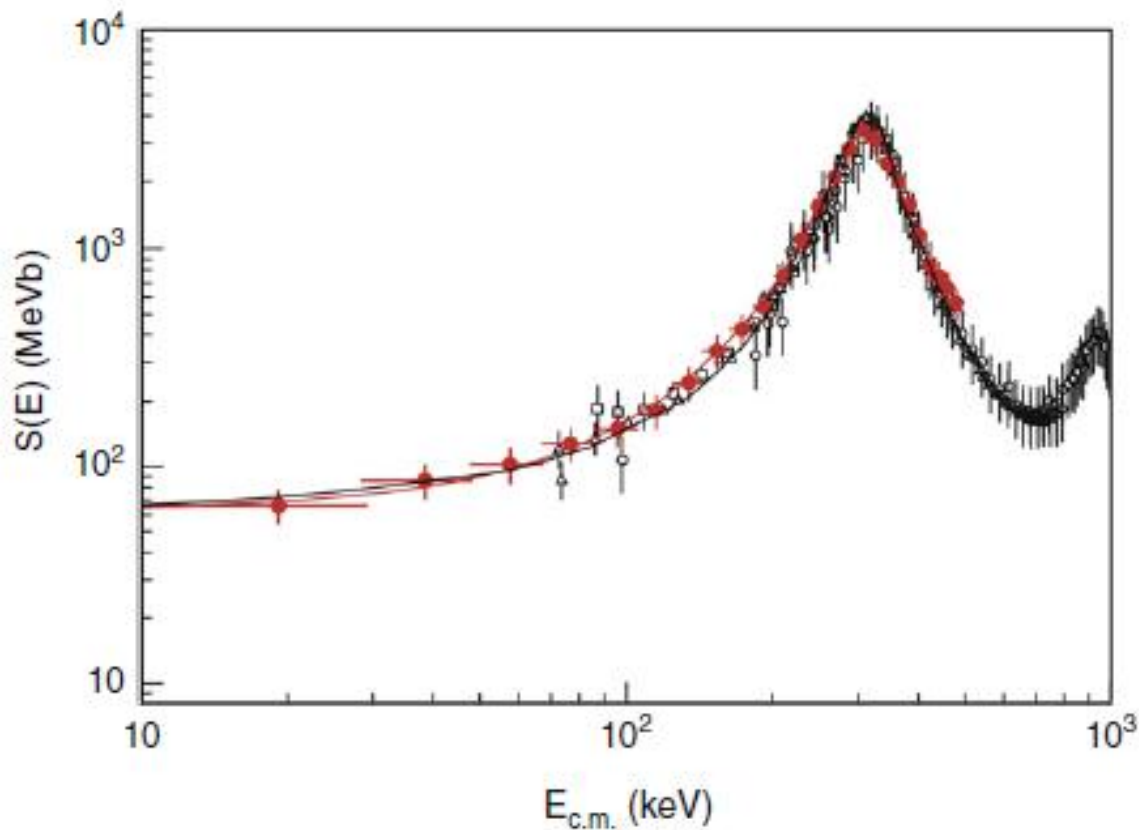
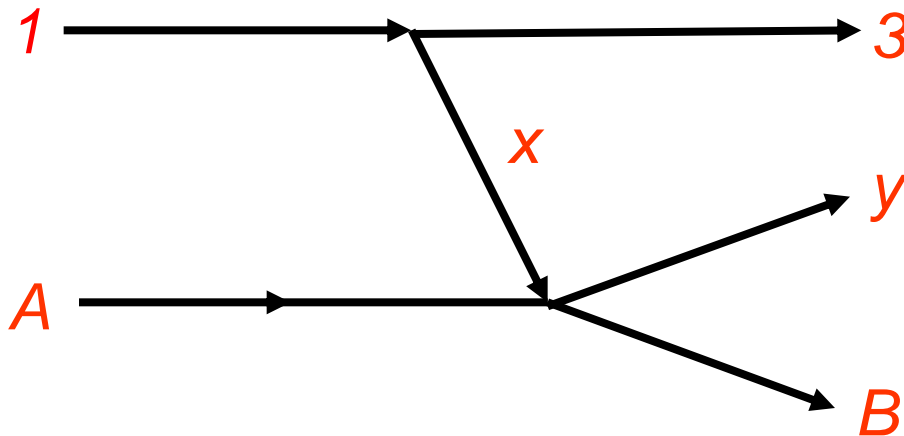


Fig. 7. S factor the $^{15}\text{N}(p,\alpha)^{12}\text{C}$ reaction obtained by the TH method using the $^{15}\text{N}(d,n\alpha)^{12}\text{C}$ reaction at $E_d = 60$ MeV (red dots). Black dots are the direct data. The black line corresponds to Breit-Wigner fit.

Other examples of astrophysical reactions for which $S(0)$ has been found by the TH method (*C. Spitaleri, A.M. Mukhamedzhanov et al., INFN-LNS, Catania, Italy*)

- ${}^7\text{Li} + p \rightarrow \alpha + \alpha$ (from $d+{}^7\text{Li} \rightarrow \alpha+\alpha+n$) ($x=p, 1=d$)
- ${}^6\text{Li} + d \rightarrow \alpha + \alpha$ (from ${}^6\text{Li}+{}^6\text{Li} \rightarrow \alpha+\alpha+\alpha$) ($x=d, 1={}^6\text{Li}$)
- ${}^6\text{Li} + p \rightarrow \alpha + {}^3\text{He}$ (from $d+{}^6\text{Li} \rightarrow \alpha+{}^3\text{He}+n$) ($x=p, 1=d$)
- ${}^{11}\text{B} + p \rightarrow {}^8\text{Be} + \alpha$ (from $d+{}^{11}\text{B} \rightarrow {}^8\text{Be}+\alpha+n$) ($x=p, 1=d$)



2. Coulomb dissociation method

Use is made of experimental data on the dissociation of a fast nucleus a in the Coulomb field of a heavy nucleus A (e.g. lead)



The cross section of that process induced by a high energy virtual photon could be related to the photoeffect cross section ($\gamma + a \rightarrow b + c$), which by the time reversal is related to the sought-for cross section of the inverse process of the radiative capture $b + c \rightarrow \gamma + a$.

Strong interaction effects could be reduced if one performs measurements at low scattering angles when the electromagnetic interaction dominates over the nuclear one.

3. Method of asymptotical normalization coefficients (ANC)

The ANC method allows one to determine $S(E \sim 0)$ for the radiative capture reactions using their peripheral character due to the Coulomb (or centrifugal) barrier.

The cross section for a nonresonant radiative-capture reaction $A(x, \gamma) B$ at zero relative energy depends only on the long-distance behavior of the $x+A$ wave function (and on the overlap of that extended wave function with B). The detailed short-range behavior of the scattering state $x + A$ or bound state B is not relevant to the reaction mechanism. At large distances the overlap integral of the wave functions of A , x , and B is

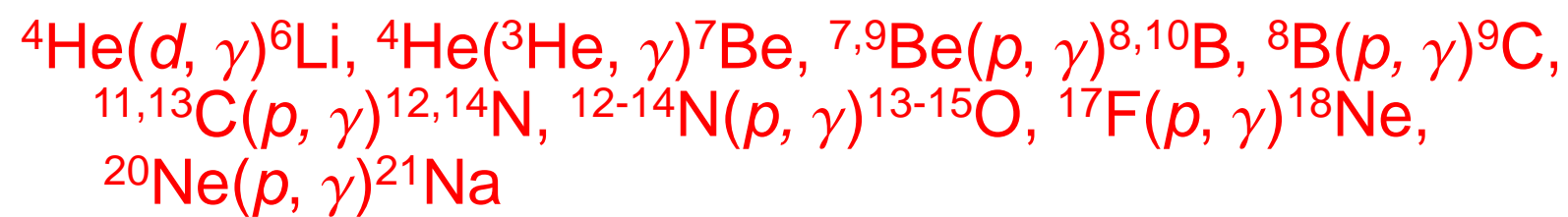
$$I_l(r) = C_1 \frac{W_{-\eta, l+1/2}(2\kappa r)}{r} \approx C_1 \frac{\exp(-\kappa r)}{(2\kappa)^\eta r^{1+\eta}} \quad (\text{charge particles } x),$$
$$I_l(r) = C_2 \frac{k_l(\kappa r)}{r} \approx C_2 \frac{\exp(-\kappa r)}{r^1} \quad (\text{neutrons}).$$
(17)

The ANCs needed for the $A(x,\gamma) B$ reaction could be found from the other nuclear reaction, the mechanism of which includes the $A+x\rightarrow B$ vertex. Usually ANCs are determined from peripheral transfer reactions using the DWBA. The particle energies in the initial and final states could be large enough.

The check of the method has been performed by comparison the experimental data for $^{16}\text{O}(^3\text{He},d)^{17}\text{F}$ and $^{16}\text{O}(p,\gamma)^{17}\text{F}$ reactions.

The ANC method was used for many radiative capture reactions. In particular, $^{10}\text{B}(^7\text{Be},^8\text{B})^9\text{Be}$ and $^{14}\text{N}(^7\text{Be},^8\text{B})^{13}\text{C}$ reactions were used to obtain the S factor $S_{17}(0)$ for the important process $^7\text{Be}(p,\gamma)^8\text{B}$.

Other examples of using the ANC method to calculate $S(E=0)$ for radiative capture processes (A.M.Mukhamedzhanov *et al.*) :



The check has been made of the sensitivity of the cross section extracted to the parameters of the optical potential within the DWBA (A.M.Mukhamedzhanov *et al.*) .

TABLE XII. Summary of updates to S values and derivatives for CNO reactions.

Reaction	Cycle	$S(0)$ keV b	$S'(0)$ b	$S''(0)$ keV ⁻¹ b
$^{12}\text{C}(p, \gamma)^{13}\text{N}$	I	1.34 ± 0.21	2.6×10^{-3}	8.3×10^{-5}
$^{13}\text{C}(p, \gamma)^{14}\text{N}$	I	7.6 ± 1.0 7.0 ± 1.5	-7.83×10^{-3}	7.29×10^{-4}
$^{14}\text{N}(p, \gamma)^{15}\text{O}$	I	1.66 ± 0.12	-3.3×10^{-3}	4.4×10^{-5}
$^{15}\text{N}(p, \alpha_0)^{12}\text{C}$	I	$(7.3 \pm 0.5) \times 10^4$	351	11
$^{15}\text{N}(p, \gamma)^{16}\text{O}$	II	36 ± 6 64 ± 6 29.8 ± 5.4		
$^{16}\text{O}(p, \gamma)^{17}\text{F}$	II	10.6 ± 0.8	-0.054	
$^{17}\text{O}(p, \alpha)^{14}\text{N}$	II		Resonances	
$^{17}\text{O}(p, \gamma)^{18}\text{F}$	III	6.2 ± 3.1	1.6×10^{-3}	-3.4×10^{-7}
$^{18}\text{O}(p, \alpha)^{15}\text{N}$	III		Resonances	
$^{18}\text{O}(p, \gamma)^{19}\text{F}$	IV	15.7 ± 2.1	3.4×10^{-4}	-2.4×10^{-6}

Nowadays for numerous astrophysical reactions $S(0)$ and its derivatives are determined by various methods (see examples in the Table). However for many important processes such data are absent, and the accuracy of the available data should be improved.

Nuclear experiments using beams of rare (unstable) isotopes

Unstable nuclei take part in many astrophysical nuclear processes (*r* process, *rp* process). Lately experiments using accelerated beams of such nuclei are performed actively.

Two main mechanisms of formation and separation of exotic nuclei

- Beams of short-lived nuclei are formed in a thin target and are separated in-flight;
- Exotic nuclei are formed and stopped in a thick target and then are extracted and accelerated anew (on-line).

Several examples of important astrophysical processes with unstable nuclei measured recently ($T_{1/2}$ in brackets):

${}^7\text{Be}(53d)(p, \gamma){}^8\text{B}$; ${}^{13}\text{N}(10m)(p, \gamma){}^{14}\text{O}$; ${}^{19}\text{Ne}(17s)(p, \gamma){}^{20}\text{Na}$; ${}^{15}\text{O}(122s)(\alpha, \gamma){}^{19}\text{Ne}$;
 ${}^{19}\text{Ne}(17s)(p, \gamma){}^{20}\text{Na}$; ${}^{18}\text{F}(110m)(p, \alpha){}^{15}\text{O}$; ${}^{14}\text{O}(71s)(\alpha, p){}^{17}\text{F}$.

Along with measuring of cross sections, measuring of masses of unstable nuclei is an important goal when dealing with radioactive beams. Two main methods of mass determination: By energy release in a reaction and by deflection of ions in electromagnetic fields.

Lately the considerable progress has been achieved in the experimental nuclear astrophysics and in developing theoretical methods of describing astrophysical processes. The further development of that field is related with creating the next generation of installations (GSI/FAIR in Germany and FRIB in the USA), as well as with modernization of acting installations GANIL in France and TRIUMF in Canada.

Analytic continuation of effective range expansion (ERE)

One of the most widespread methods is the analytic continuation in energy of the data on the partial wave amplitude of elastic BC scattering to the pole corresponding to the bound state A . The most effective way of realization of this procedure is the analytic continuation of the effective range function $K_L(k_2)$. This method was used (L.B., V.I.Kukulin et al.) to obtain S wave VC s and ANC s for the process ${}^6\text{Li} \rightarrow \alpha + d$, by Yu.V.Orlov et al. for the systems ${}^3\text{H}$, ${}^2;{}^3;{}^5\text{He}$, ${}^5\text{Li}$, ${}^8\text{Be}$, and by J.-M.Sparenberg et al. for the systems ${}^{16}\text{O} + n$, ${}^{16}\text{O} + p$, and ${}^{12}\text{C} + \alpha$.

All above works treated one-channel elastic scattering. However, the description of scattering of particles with nonzero spins even in the absence of inelastic channels often demands account of channel coupling. The most typical situation induced by tensor forces is the case of two coupled channels 1 and 2 with the same J but different L (L_1 and $L_2 = L_1 + 2$). Examples: $d\alpha$ scattering, NN triplet scattering etc. In principle, coupled channels may differ not in L but in channel spins.

In the work [1] (L.B., *Yad. Fiz.*, 2011. V.74. P.1008) it was considered the generalization of the ERE to the case of two coupled channels and using that expansion for the determination of VCs and ANCs. The consideration in [1] was carried out for the short-range interaction, which practically limited using the formalism developed to the reactions induced by neutrons. Now the results of [1] are generalized to account of the Coulomb interaction which radically changes analytic properties of scattering amplitudes and their behavior at low energies.

The formalism developed could be applied to any two-channel nuclear system, for which the results of the phase-shift analysis are known (including the mixing parameter). One of similar important systems is ${}^6\text{Li}$ in the $\alpha + d$ channel. The ANC values for this system determine the cross section of the radiative capture ${}^4\text{He}(d,\gamma){}^6\text{Li}$, which is the main process of ${}^6\text{Li}$ formation in the big bang model. Direct measurements of that process at astrophysical energies are absent due to the smallness of the cross section. The data on the values of the VCs and ANCs for ${}^6\text{Li} \rightarrow \alpha + d$ ($L=0; 2$) channel obtained by different methods are characterized by a large spread. In the first place it refers to the D -state constants.

The procedure of analytic continuation of the two-channel ERE described above has been applied to $d\alpha$ scattering using several sets of phase shifts (L.B. and D.A.Savin). The values of the VCs and ANCs for ${}^6\text{Li} \rightarrow \alpha + d$ ($L = 0; 2$) were extracted.

Using the data from the available phase-shifts analysis results in $G_0^2 = 0.4 - 0.5 \text{ fm}; C_0 = 2.3 - 2.8 \text{ fm}^{-1/2}$.

Solution of Faddeev equations (neglecting the Coulomb interaction) gives

$$G_0^2 = 0.3 \text{ fm}; C_0 = 2.0 \text{ fm}^{-1/2}$$

Low accuracy of phase-shift analysis at low energies and simplicity of Faddeev equations used did not let to obtain accurate values of VC and ANC for $L = 2$.

$$C_2 = 0.02 - 0.05 \text{ fm}^{-1/2}$$

Including inelastic channels

The procedure described above considers elastic channels only. On the other hand, low-lying inelastic thresholds might influence the **ERE**. The simplest way to allow for inelastic channels is to include into the **ERE** an additional term, which is complex at energies above an inelastic threshold.

To guarantee that this procedure leads to the correct analytic behavior of scattering amplitudes at the threshold $E = E_0$, one may choose that term proportional to $(E - E_0)^{1/2}$ in case of a **two**-particle threshold and to $(E - E_0)^2 \ln(E - E_0)$ in case of a **three**-particle threshold.

We plan to apply that procedure to the $d\alpha$ scattering.

Thank you